OPEN ACCESS Freely available online

PLoS GENETICS

Genetic Regulation by NLA and MicroRNA827 for Maintaining Nitrate-Dependent Phosphate Homeostasis in *Arabidopsis*

Surya Kant[1], Mingsheng Peng[1,2], Steven J. Rothstein[1]*

1 Department of Molecular and Cellular Biology, University of Guelph, Guelph, Canada, **2** Monsanto Company, Chesterfield, Missouri, United States of America

Abstract

Plants need abundant nitrogen and phosphorus for higher yield. Improving plant genetics for higher nitrogen and phosphorus use efficiency would save potentially billions of dollars annually on fertilizers and reduce global environmental pollution. This will require knowledge of molecular regulators for maintaining homeostasis of these nutrients in plants. Previously, we reported that the *NITROGEN LIMITATION ADAPTATION* (*NLA)* gene is involved in adaptive responses to low-nitrogen conditions in *Arabidopsis*, where *nla* mutant plants display abrupt early senescence. To understand the molecular mechanisms underlying *NLA* function, two suppressors of the *nla* mutation were isolated that recover the *nla* mutant phenotype to wild type. Map-based cloning identified these suppressors as the phosphate (Pi) transport-related genes *PHF1* and *PHT1.1*. In addition, *NLA* expression is shown to be regulated by the low-Pi induced microRNA miR827. Pi analysis revealed that the early senescence in *nla* mutant plants was due to Pi toxicity. These plants accumulated over five times the normal Pi content in shoots specifically under low nitrate and high Pi but not under high nitrate conditions. Also the Pi overaccumulator *pho2* mutant shows Pi toxicity in a nitrate-dependent manner similar to the *nla* mutant. Further, the nitrate and Pi levels are shown to have an antagonistic crosstalk as displayed by their differential effects on flowering time. The results demonstrate that *NLA* and miR827 have pivotal roles in regulating Pi homeostasis in plants in a nitrate-dependent fashion.

Citation: Kant S, Peng M, Rothstein SJ (2011) Genetic Regulation by NLA and MicroRNA827 for Maintaining Nitrate-Dependent Phosphate Homeostasis in *Arabidopsis*. PLoS Genet 7(3): e1002021. doi:10.1371/journal.pgen.1002021

Editor: Li-Jia Qu, Peking University, China

Received November 7, 2010; **Accepted** January 21, 2011; **Published** March 24, 2011

Funding: This work was supported by grants from the Natural Sciences and Engineering Research Council of Canada and Ontario Research Fund to SJR. The funders had no role in study design, data collection and analysis, decision to publish, or preparation of the manuscript.

Competing Interests: The authors have declared that no competing interests exist.

* E-mail: rothstei@uoguelph.ca

Introduction

High yielding crops require the application of large amounts of nitrogen (N) and phosphorus (P) fertilizers. However, most of the crop plants are able to take up less than 40% of the applied N and P fertilizers and the rest of it is lost to the environment. This leads to an increase in crop production cost and significant global environmental damage by eutrophication of marine and fresh water ecosystems and gaseous loss to the atmosphere [1–3]. For instance, a 1% increase in N use efficiency worldwide would save ~$1.1 billion annually. In addition, a ~2.5-fold increase in N- and P-driven eutrophication of water bodies is expected by the year 2050 given current trends [1]. Therefore, developing crop varieties with higher nutrient use efficiency to restrict the excessive use of N and P fertilizer is required. For this, a comprehensive knowledge of molecular mechanisms regulating N and P homeostasis in plants is a prerequisite.

P is an essential structural component of nucleic acids and phospholipids and is a key constituent of high energy phosphate compounds such as ATP and ADP [2]. Despite the integral role of P for normal plant growth, development and yield, P availability in soil is usually the lowest of the macronutrients [4]. Even though the total P content in soil is high, its availability for plant uptake is largely restricted due to its adsorption in soil, precipitation by other cations and conversion into organic forms by microbes [2,5]. To maintain internal P homeostasis, plants have evolved a series of adaptive responses that include induction of inorganic phosphate (Pi) transporters, change of root architecture, secretion of phosphatase and symbiosis with mycorrhizal fungi [1,5,6]. Genetic and molecular approaches have revealed several genes involved in Pi transport, homeostasis and adaptive responses in plants [6]. Among the regulatory genes for Pi homeostasis, *PHOSPHATE STARVATION RESPONSE1* (*PHR1*) is a MYB transcription factor which acts in the Pi starvation signaling pathway by regulating a group of Pi starvation induced genes [7]. PHR1 has sumoylation sites and is a target of the SUMO E3 ligase SIZ1 which is a controller of Pi starvation dependent responses in *Arabidopsis* [8]. A SEC12-related *PHOSPHATE TRANSPORTER TRAFFIC FACILITATOR1* (*PHF1*) gene facilitates the trafficking of a key high affinity Pi transporter, *PHOSPHATE TRANSPORTER1.1* (*PHT1.1*), which is involved in Pi acquisition [9,10]. The *pht1.1* mutant shows reduced Pi uptake in *Arabidopsis* [10] and its overexpression increased the Pi uptake in tobacco cells [11]. Another Pi transporter *PHT1.4* might have a role in Pi uptake under high Pi conditions and a *pht1.1* x *pht1.4* double mutant shows a significant reduction in Pi uptake and shoot Pi content [10]. The low affinity Pi transporter *PHT2.1* facilitates Pi allocation within the plant between roots and shoots and is required for Pi remobilization in old and young leaves [12]. Twenty genes with SPX domains (SYG1, Pho81 and XPR1)

Author Summary

Higher crop yields require increased use of fertilizers, especially for the prime macronutrients nitrogen and phosphorus. Increasing nitrogen and phosphorus use efficiency in plants would decrease crop production cost and reduce environmental pollution. In an attempt to isolate the regulatory genes for nitrogen and phosphorus homeostasis in plants, we identified the *NLA* gene as having a role in plant adaptation under low-nitrogen conditions. In the current work, detailed genetic and molecular analysis for the functionality of this gene revealed that *NLA* has a key role in the maintenance of phosphate (Pi) homeostasis in plants in a nitrate-dependent fashion. Further, Pi has an antagonistic crosstalk with nitrate, not only with regards to its accumulation, but also in its differential effects on flowering time. Interestingly, the antagonistic genetic interaction of Pi is with nitrate, but not with ammonium.

respond to Pi levels and SPX1 and SPX3 are proposed to regulate the expression of Pi starvation response genes [13]. Another SPX-domain containing gene *PHO1* has a role in Pi loading into the xylem and possibly also in Pi signaling [14,15]. The *pho1* mutant has significantly lower levels of shoot Pi, but has normal root Pi content [14,16]. A mutation in a ubiquitin conjugase gene *PHO2* results in overaccumulation of Pi that causes Pi toxicity in *Arabidopsis* [17,18]. The *PHO2* gene is a target of the microRNA, miR399 [18,19]. Like other nutrient elements, uptake of Pi also depends upon external pH and ion competition. At low pH, Pi in the $H_2PO_4^-$ form is present at a high proportion whereas at high pH HPO_4^{2-} dominates [2]. Competition between Pi and arsenate is well known and both are taken up by the same transport system [2,9].

N components are not only required for plant growth, but also serve as regulators of various metabolic and developmental pathways. Plants take up N mainly as nitrate (NO_3^-) and ammonium (NH_4^+), with NO_3^- being the predominant form in most agricultural soils [20]. NO_3^- and Pi are the two most important anions required for plant growth and development. However, the interaction and balance between NO_3^- and Pi in plants is not well studied. Here, we demonstrate the crosstalk between NO_3^- and Pi and the role of genes encoding an E3 ubiquitin ligase, *NITROGEN LIMITATION ADAPTATION* (*NLA*) and an E2 ubiquitin conjugase, *PHO2*, and a microRNA- miR827, in maintaining Pi homeostasis in *Arabidopsis thaliana* in a NO_3^- dependent manner.

Results

Identification of the *nla* Mutant and *nla*-Suppressors, *phf1* and *pht1.1*

The *nla* mutant was identified based on its altered growth response to N limitation. *nla* mutant plants failed to show several adaptive responses to low-N conditions, such as the inability to accumulate anthocyanin and abrupt early senescence compared to wild type (WT) plants [21]. The *nla* phenotype was specific to the low-N growth condition, since at optimum-N and under other abiotic stresses, both *nla* and WT plants were similar in phenotype [21]. Later, it was revealed that in *nla* mutant plants under low-N conditions, the substrate in phenylpropanoid pathway was channeled towards lignin biosynthesis instead of anthocyanin synthesis, resulting in low anthocyanin accumulation [22]. Anthocyanin protects plants from photoinhibition damage under various stress conditions [22,23]. A lack of anthocyanin accumulation in the *nla* mutant under low-N conditions means an absence of the photo-protective screen, which might result in the early senescence phenotype in *nla* mutant plants.

This evidence suggests that the *NLA* gene regulates the *Arabidopsis* adaptive responses under low-N. The knowledge of N regulatory genes is limited and the *NLA* gene might be a key component for the regulation of plant adaptation to low-N. Therefore, we initiated further studies to understand in more detail the physiological and molecular role of *NLA*. One approach was to generate and identify suppressor mutations in the *nla* mutant, which would restore the *nla* mutant phenotype to WT. For this *nla* mutant seeds were chemically mutagenised and screened at low-N supply. Two suppressor plants (*nla-sup1* and *nla-sup2*) were identified which were phenotypically similar to WT in that the *nla*-suppressor plants did not show early senescence under low-N conditions (Figure 1A, 1B and Figure S1A, S1B). These suppressor genes were identified separately using map-based cloning approaches. The *nla-sup1* locus was mapped to the lower arm of chromosome 3, in a ~132 kb region with 40 annotated genes (Figure 1C). Sequencing this genomic region for each gene revealed that in *PHF1* (At3g52190) a transition of a single G/C to A/T occurred at the 3′ end of intron 7 (position 2218). This transition destroyed the conserved dinucleotide, 'AG', which is required for proper splice recognition at the 3′ end of an intron. The resulting altered splice site led to the inclusion of the adjacent exonic 'G' as part of the intron (Figure 1C) leading to a 1 bp deletion in the processed mRNA. The cDNA sequence also revealed that in the *nla-sup1* one 'G' nucleotide was missing compared to WT which causes a frameshift and generation of a premature stop codon resulting in a truncated PHF1 protein sequence (Figure 1C). The second suppressor, *nla-sup2*, was mapped to a location on chromosome 5. Sequencing of the genomic regions confirmed a mutation in a single G/C to A/T (position 229) in the first exon of *PHT1.1* (At5g43350) gene. This transition results in a switch from alanine to threonine (position 73) in the amino acid sequence of the PHT1.1 protein (Figure 1D). *PHT1.1* is a high affinity Pi uptake transporter [10] and *PHF1* facilitates the trafficking of *PHT1.1* [9]. To confirm that these altered genes corresponded to the suppressor mutations, their respective T-DNA insertion mutants were used to make *nla* x *phf1* and *nla* x *pht1.1* double mutants. Like the suppressor mutations, these double mutants also recovered the *nla* mutant phenotype to WT.

MicroRNA827 Suppresses the *NLA* Transcript Level

MicroRNAs (miRNAs) are noncoding small RNAs and suppress the expression of genes that have nearly complementary sequences by mRNA cleavage [24,25]. The *NLA* gene is a putative target of a miRNA, miR827 (At3g59884) based on complementary sequences (Figure 2A and 2B). By identifying *phf1* and *pht1.1* as *nla*-suppressors, we have shown that *NLA* directly or indirectly targets *PHF1* and *PHT1.1*. To know how *NLA* expression is regulated and whether the *NLA* transcript is a target of miR827, we analyzed the expression pattern of *NLA* and miR827 under different N and Pi regimes. Also the expression of *NLA* transcript was analyzed in the miR827 overexpresser (OX) and T-DNA mutant lines. The expression of miR827 is up-regulated by low-Pi conditions (Figure 2C) [26]. In contrast, the transcript level of *NLA* was down-regulated under low-Pi, the exact opposite response to the expression of miR827 (Figure 2D). Figure 2E shows that miR827 was overexpressed by 35-times in the OX-miR827 line and there was very low expression in the miR827-mutant plants as compared to WT. The *NLA* transcript level was over 3-fold

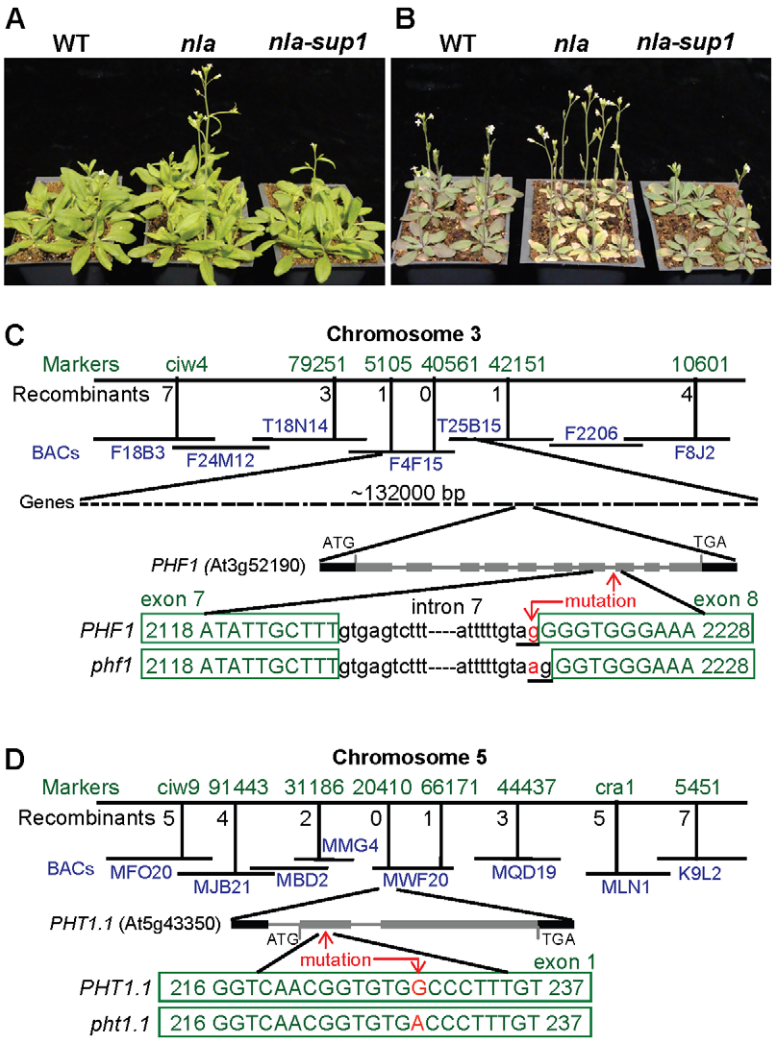

Figure 1. Recovery of the *nla* mutant phenotype by *nla-suppressor1* and mapping of the *nla*-suppressors, *PHF1* and *PHT1.1*. (A) WT, *nla* and *nla-sup1* (*nla-phf1*) plants grown at 10 mM NO_3^--10 mM Pi. (B) Plants grown at 3 mM NO_3^--10 mM Pi. (C) Mapping and partial genomic sequence of WT and *nla-sup1* (*phf1*). The transition at 3′ end nucleotide 'g' to 'a', indicated by red arrow, disrupted the conserved dinucleotide, AG (underlined), which is required for splicing. In the *phf1* mutation, the next available 'G' from the 5′ end of exon became part of the intron to form 'AG', causing loss of one G from the *phf1* coding sequence. This cryptic splice site resulted in a frameshift and creation of a premature stop codon. (D) The mutation in the second *nla* suppressor was missense in *PHT1.1* gene. In the first exon, nucleotide 'G' at position 229 was switched to 'A' which changes the codon GCC (encodes alanine) to ACC (for threonine).
doi:10.1371/journal.pgen.1002021.g001

down-regulated in the OX-miR827 and over 2-fold up-regulated in miR827 mutant plants compared to WT (Figure 2F). These results show that *NLA* is a target of miR827. Similarly, the *PHO2* gene has been reported to be a target of miR399 and their expression level is also Pi dependent [18,19].

The *nla* Mutant Overaccumulates Pi in Shoots Specifically at Low NO_3^- Supply

It has been shown previously that *phf1* and *pht1.1* mutants accumulate less Pi than WT [9,10]. Therefore, the identification of the *nla*-suppressors as *phf1* and *pht1.1* mutations (Figure 1) and the transcript change of *NLA* with Pi levels (Figure 2C) indicate that Pi accumulation in the *nla* mutant might be impaired. Pi analysis reveals that under sufficient N-P conditions of 10 mM NO_3^--10 mM Pi, where the *nla* mutant is phenotypically similar to WT (Figure 1A), Pi content in the *nla* mutant shoots was ~1.8-fold higher than WT (Table 1). Interestingly, under the relatively low NO_3^- (3 mM NO_3^--10 mM Pi) regime where the *nla* mutant shows early senescence (Figure 1B), Pi content in the *nla* mutant shoots increased ~6.6-fold compared to WT (Table 1). P usually makes up ~0.2% of plant dry matter and visual symptoms of Pi toxicity appear when P constitutes >1% of dry matter [2,27]. Pi content in the *nla* mutant shoots at 3 mM NO_3^--10 mM Pi regime makes up ~2% of dry matter and its senescence phenotype likely is due to Pi toxicity, which leads to chlorosis or necrosis starting from the leaf margins (Figure 1B). Whereas, the *nla* mutant grown at low-Pi regimes accumulated Pi below P toxicity limits (Table 1). Also the *nla* suppressors, *nla-sup1* and *nla-sup2* as well as OX-*NLA* had a visual phenotype and Pi content similar to WT (Figure 1, Figure S1 and Table 1). Interestingly, the previously described Pi overaccumulator, *pho2* mutant [17,28], shows a phenotype and Pi content similar to the *nla* mutant (Table 1, Figure S1C and S1D). Pi toxicity in the *nla* and *pho2* mutants was evident only when NO_3^- supply was relatively low with plants grown on 3 mM NO_3^--10 mM Pi, while at the 10 mM NO_3^--10 mM Pi regime the plants were phenotypically similar to WT

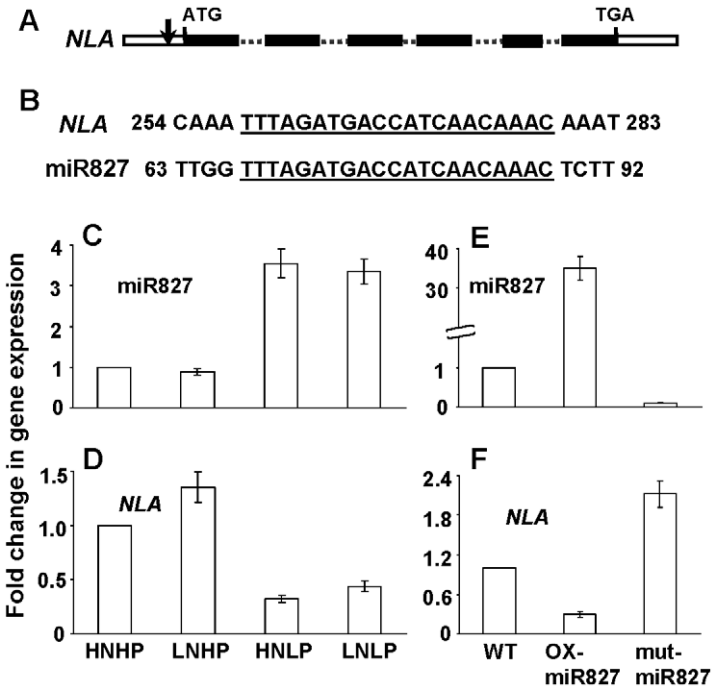

Figure 2. Regulation of *NLA* expression by miR827. (A) *NLA* gene organization, exons (black boxes), introns (dotted lines), and UTR (empty boxes). Arrow indicates putative target site of miR827. (B) Partial sequences of *NLA* and miR827, the complementary sequences are underlined. (C) Relative expression of miR827, and (D) *NLA* in WT plants grown at HNHP (10 mM NO_3^--10 mM Pi), LNHP (3 mM NO_3^--10 mM Pi), HNLP (10 mM NO_3^--0.5 mM Pi), and LNLP (3 mM NO_3^--0.5 mM Pi). (E) Relative expression of miR827, and (F) *NLA* in WT, miR827-overexpressor, and miR827-mutant plants grown at 10 mM NO_3^--10 mM Pi conditions. Expression levels were determined by real-time PCR. Shown are mean ± SD.
doi:10.1371/journal.pgen.1002021.g002

(Figure S1C and S1D). This led to the obvious assumption that NO_3^- is also playing a role in Pi accumulation. This crosstalk is evident when Pi supply was constant and NO_3^- supplies were variable, where Pi content in WT shoots increased with decreasing NO_3^- applications (Table 1 and Table 2). In the *nla* and *pho2* mutants, Pi accumulation accelerated and the appearance of Pi toxicity symptoms occurred earlier in accordance with decreasing NO_3^- supply at a given Pi level (Table 2). Pi toxicity in these mutants occurred only under low NO_3^- availability. This can be ascribed to the additive effects of lack of negative regulation by *NLA* or *PHO2* and minimal suppression of NO_3^- on Pi accumulation.

The Pi toxicity symptom in the *nla* mutant appears mainly after bolting [21] and the above results are from plants at 27 days after sowing (DAS) when plants were already flowering. Therefore, Pi contents at the initiation of bolting (22 DAS) and before bolting (17 DAS) were also analyzed (Table S1). Pi accumulation at 22 and 17 DAS followed a similar trend to that of 27 DAS under varying NO_3^--Pi regimes. However, net Pi accumulation in shoots at a specific NO_3^--Pi regime was much lower at 17 DAS than 27 DAS (Table S1 and Table 1) and the *nla* mutant did not show Pi toxicity before bolting. This indicates that the accumulation of Pi accelerates with the transition of *Arabidopsis* from the vegetative to the reproductive stage. The roots are the initial sites of contact with Pi, but root growth and architecture are similar between *nla* and WT at varying NO_3^--Pi regimes [21]. In conjunction with this, at low NO_3^- availability the fold differences for Pi content in roots of the *nla* mutant vs WT was much less than that observed in shoots (Table S2 and Table S3). This suggests that most of the Pi taken up by roots was not retained by them, but was transported towards the shoots.

A radiolabelled ^{33}Pi uptake assay was conducted to assess whether the overaccumulation of Pi in the *nla* and *pho2* mutants was due to increased Pi uptake. Indeed, the *nla* and *pho2* mutants showed a higher ^{33}Pi uptake rate than WT, *nla-sup1*, *nla-sup2* and

Table 1. Pi content in *Arabidopsis* shoots (nmole/mg fresh weight).

Treatment	WT	*nla*	*pho2*	*nla-sup1*	*nla-sup2*	OX-*NLA*
NO_3^--Pi (mM)						
10-10	17.3±1.9gh	30.9±3.1bc	35.2±3.2b	10.6±1.1i	16.9±1.8gh	15.6±1.4h
3-10	28.7±2.9cd	191±23.1a	203±22.3a	19.9±1.7fg	36.4±4.1b	24.2±2.1de
10-0.5	3.1±0.3m	7.3±0.9k	8.4±0.8jk	2.6±0.3n	3.8±0.3l	2.7±0.2n
3-0.5	9.1±1.1ij	21.4±1.9ef	24.2±2.3de	7.2±0.7k	10.6±1.2i	8.2±0.9jk

Pi content was measured at 27 days after sowing. Shown are mean ± SD. Values with different letters indicate significant difference at $P<0.05$.
doi:10.1371/journal.pgen.1002021.t001

Table 2. Pi content (nmole/mg fresh weight) and Pi toxicity in *Arabidopsis* shoots.

Treatment NO_3^--Pi (mM)	WT	*nla*	*pho2*	Pi toxicity in *nla* and *pho2*
	Pi content			
10-10	16.8±1.4kl	30.2±3.1fg	34.9±3.5ef	No
3-10	28.1±2.2gh	189±17.4b	199±21.2b	24 DAS
1-10	32.1±3.1fg	246±21.2a	254±24.2a	19 DAS
10-3	12.1±1.1m	22.4±2.1i	24.8±2.3hi	No
3-3	20.4±1.9ij	75.4±6.8d	80.4±8.2d	26 DAS
1-3	23.3±2.0i	212±21.2ab	220±21.8ab	20 DAS
10-1	7.5±0.8n	15.7±1.6kl	17.8±1.9jk	No
3-1	15.3±1.2l	35.4±3.3ef	39.6±3.5e	No
1-1	18.7±1.5jk	112±10.4c	116±11.5c	25 DAS

Pi content was measured at 27 days after sowing (DAS). Pi toxicity was recorded as the day when leaves of >50% plants start to show Pi toxicity symptoms. The WT plants did not show Pi toxicity. Shown are mean ± SD. Values with different letters indicate significant difference at $P<0.05$.
doi:10.1371/journal.pgen.1002021.t002

OX-*NLA* plants (Figure 3). NLA is an E3 Ubiquitin Ligase and has two distinct domains, SPX and RING. The *nla* is a deletion mutation (Col background) with a disrupted RING domain [21]. To ascertain if a different type of *nla* mutation would exert similar effects, a T-DNA insertion mutant in the same gene but in the ecotype Wassilewskija (Ws) (FLAG_352A03) was obtained. The *nla* mutant (Ws background) showed a similar Pi toxicity phenotype and Pi content as that of the *nla* mutant (Col background) under low NO_3^--high Pi conditions (Figure S3).

For the detailed analysis of Pi homeostasis maintenance and the complementation study, several overexpresser (Table 3A) and double mutant (Table 3, Double Mutants) lines were generated. As shown above, miR827 suppresses *NLA* expression (Figure 2F). Indeed, Pi content in the OX-miR827 plants was ~6.4-fold higher than WT. Pi toxicity and Pi content were similar in OX-miR827 and *nla* mutant plants. Whereas, the miR827 mutant had Pi content similar to the OX-*NLA* plants (Table 3). The *PHF1* gene facilitates the trafficking of the key Pi uptake transporter, *PHT1.1*, and their mutant lines had lower Pi content than WT (Table 3C). Hence, their overexpression lines would be expected to accumulate higher Pi and might show Pi toxicity, as observed in the *nla*

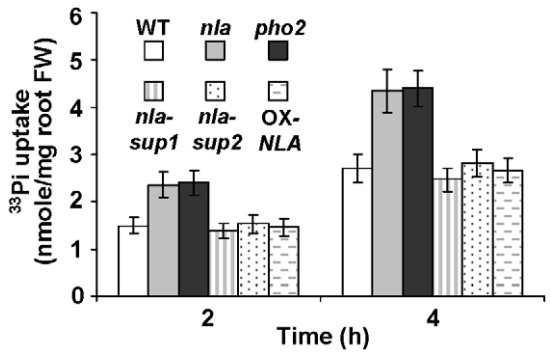

Figure 3. ^{33}Pi uptake activities in *Arabidopsis* plants. Shown are mean ± SD ($n=10$). (FW) Fresh weight.
doi:10.1371/journal.pgen.1002021.g003

Table 3. Inorganic phosphate (Pi) and total phosphorus (P) contents in *Arabidopsis* shoots (nmole/mg fresh weight).

Genotype	Pi	Total P
Overexpresser lines		
WT OX-*NLA*	23.1±2.0ef	57.9±6.2ef
WT OX-miR827	175±18.2ab	419±38.2ab
WT OX-*PHF1*	42.7±3.5c	107±11.4c
WT OX-*PHT1.1*	40.2±3.9cd	101±10.1cd
nla-sup1 OX-*PHF1*	180±16.8a	437±46.2a
nla-sup1 OX-*NLA*	10.2±1.1i	33.8±3.1h
nla-sup2 OX-*PHT1.1*	167±15.2ab	416±39.8ab
nla-sup2 OX-*NLA*	18.4±1.9g	47.2±5.1fg
nla OX-*PHF1*	189±20.1a	450±43.7a
nla OX-*PHT1.1*	188±19.8a	446±42.2a
pho2 OX-*PHF1*	192±21.2a	453±40.4a
pho2 OX-*PHT1.1*	190±20.1a	450±42.5a
Double mutants		
nla x *pho2*	200±19.1a	474±50.2a
nla x *phf1*	21.2±1.9fg	57.5±5.5ef
nla x *pht1.1*	37.5±3.2cd	95.2±8.9cd
nla x *pht1.4*	174±18.2ab	425±46.5ab
nla x *pht2.1*	171±17.4ab	417±38.4ab
nla x *pho1*	10.2±1.2i	31.1±2.7h
nla x *phr1*	146±15.9b	357±32.3b
nla x *siz1*	179±18.8ab	427±40.2ab
pho2 x *phf1*	23.4±2.1ef	62.2±6.6e
pho2 x *pht1.1*	35.2±2.9cd	91.5±10.2cd
Control plants		
WT	27.4±2.2e	67.8±6.6e
nla	186±19.2a	441±42.2a
pho2	197±21.2a	461±48.4a
mut-miR827	23.7±1.9ef	59.1±5.5ef
nla-sup1	20.7±2.0fg	53.6±5.1ef
nla-sup2	39.7±4.1cd	99.6±10.9cd
phf1	12.8±1.2h	41.2±3.9g
pht1.1	17.2±1.9g	46.2±5.1fg
pht1.4	26.6±3.1e	65.9±6.2e
pht2.1	25.6±2.8ef	66.2±7.1e
pho1	7.5±0.9j	24.3±2.2i
phr1	20.6±1.6fg	52.6±5.6ef
siz1	33.9±2.7d	86.1±9.1d

Plants were grown at 3 mM NO_3^--10 mM Pi and harvested at 27 days after sowing. Shown are mean ± SD. Values with different letters in each column indicate significant difference at $P<0.05$.
doi:10.1371/journal.pgen.1002021.t003

and *pho2* mutants. However, the increase in Pi content in OX-*PHF1* and OX-*PHT1.1* lines was only ~1.5-fold compared to WT, much lower than the Pi toxicity limit (Table 3A). Further, to confirm that *phf1* and *pht1.1* are *nla-sup1* and *nla-sup2* suppressor mutations, respectively, the WT cDNAs of *PHF1* and *PHT1.1* driven by the cauliflower mosaic virus 35S promoter (35S) were transformed into *nla-sup1* and *nla-sup2* mutants, respectively. The transformed *nla-sup1*-OX-*PHF1* and *nla-sup2*-OX-*PHT1.1* plants

(generated using the genomic sequences of *PHF1* and *PHT1.1*, respectively) grown at low NO_3^- had Pi content similar to the *nla* mutant (Table 3). In addition, the *nla* mutant was crossed with T-DNA mutants of *phf1* and *pht1.1*. The double mutants, *nla* x *phf1* and *nla* x *pht1.1* had Pi contents similar to *nla-sup1* and *nla-sup2*, respectively (Table 3, Double Mutants and Control Plants). The *nla* and *pho2* plants were transformed with 35S:*PHF1* and 35S:*PHT1.1*. However, these OX lines had no further increase of Pi contents over *nla* and *pho2* mutants (Table 3). The *nla* x *pho2* double mutant had no significant additive increase of Pi content compared to *nla* or *pho2* mutants (Table 3). This indicates overlapping roles of *nla* and *pho2* in Pi overaccumulation and their involvement in the same functional pathway. This is further confirmed in that *pho2* x *phf1* and *pho2* x *pht1.1* also restored Pi content to WT levels, like that of *nla* x *phf1* and *nla* x *pht1.1*, respectively (Table 3, Double Mutants). *PHT1.4* and *PHT2.1* are also Pi transporters, but their mutants had Pi content similar to WT under high Pi conditions (Table 3, Control Plants), suggesting they may have roles in Pi reallocation within plants [6,10,12]. In agreement, *nla* x *pht1.4* and *nla* x *pht2.1* double mutants accumulated high Pi levels (Table 3, Double Mutants). The *PHO1* gene is involved in Pi loading to the xylem [14] and the *pho1* mutant shoots have very low Pi content (Table 3, Control Plants) [14]. The *nla* x *pho1* double mutant gave expected results of having very low shoot Pi content compared to WT (Table 3, Double Mutants), showing that the *pho1* mutation is able to restrict Pi loading for transport from roots towards shoots in the *nla* mutant. *PHR1* regulates expression of some Pi-responsive genes [7]. The *phr1* mutant had lower shoot Pi content than WT. Also the *nla* x *phr1* mutant had a decrease in Pi content compared to the *nla* mutant (Table 3, Double Mutants and Control Plants), but not enough to avoid Pi toxicity. *SIZ1* gene encodes a SUMO E3 ligase, mutation of which had slightly higher Pi content than WT (Table 3, Control Plants) [8]. However, *nla* x *siz1* had no further increase in Pi levels over the *nla* mutant (Table 3, Control Plants).

NO_3^- and Pi Have an Antagonistic Interaction

Accumulation of Pi increased with decreasing NO_3^- supply (Table 1). The N content was analyzed to confirm whether the changing Pi application would also exert similar suppression on N accumulation. In fact, N content increased with decreasing Pi supply (Table S4). However, the suppression by Pi on N accumulation was quite low (Table S4) compared to the suppression by NO_3^- on Pi accumulation (Table 1). The differential suppression by these ions could be ascribed to their contrasting mobility in soil, given that NO_3^- diffusion is 3–4 times faster than Pi [29]. N is available in both anionic and cationic forms, NO_3^- and NH_4^+, respectively, with NO_3^- being dominant in most soils and also the preferred form taken up by most plants, including *Arabidopsis* [20]. To analyze whether the antagonistic interaction of Pi was generalized to both NO_3^- and NH_4^+, the plants were grown in different NH_4^+-Pi regimes. Surprisingly, even at high NH_4^+ supply, Pi accumulation was much higher in *nla* and *pho2* mutants (Table 4) and these mutant plants showed Pi toxicity (Figure S4). In contrast to this, equimolar concentration of NO_3^- suppressed Pi accumulation below toxicity limits in the *nla* and *pho2* mutants (Table 1, Figure 1 and Figure S1). This suggests that Pi has an antagonistic crosstalk with NO_3^-, but not with NH_4^+.

Another important finding was the interaction between the NO_3^- and Pi applications for their effect on flowering time in *Arabidopsis*. For this, the plants were grown under varying relative supplies of NO_3^- and Pi as described in the materials and methods. Plants flowered earlier when grown under low NO_3^- compared to high NO_3^- conditions. In contrast, growth with low-Pi delayed flowering compared to high Pi. Further, the interaction between these two nutrients had a cumulative effect given that the plants grown at 3 mM NO_3^--10 mM Pi flowered significantly earlier than plants at 10 mM NO_3^--3 mM Pi (Figure 4A, Figure S2). In addition, the *nla* mutant, which had higher Pi accumulation, flowered significantly earlier compared to the *phf1* mutant which had low Pi accumulation (Figure 4A). Expression levels of various genes which regulate flowering time in *Arabidopsis* were also changed in a similar fashion by NO_3^--Pi levels. *FLOWERING LOCUS C* (*FLC*) is a floral repressor [30] and its expression was lowest at 3 mM NO_3^--10 mM, where plants flowered earliest. Further, the expression of *FLC* was lower in *nla* mutant leaves than in *phf1* (Figure 4B). *FLOWERING LOCUS T (FT)*, *LEAFY* (*LFY*) and *APETALA1* (*AP1*) are positive regulators of flowering time [30], and their expression was significantly higher in leaves of plants grown on the 3 mM NO_3^--10 mM Pi than at 10 mM NO_3^--3 mM Pi. Also the expression of these genes was higher in the *nla* than in the *phf1* mutant (Figure 4C–4E). The effect of varying NO_3^- and Pi regimes on change of expression of *FLC*, *FT*, *LFY* and *AP1* genes indicates that the autonomous and gibberellin pathways for flowering are affected. Since, Pi and gibberellin levels are positively correlated in *Arabidopsis* [31] and gibberellin is known to promote flowering [32], which was reflected by early flowering at high Pi content (Figure 4A).

Table 4. Pi content in *Arabidopsis* shoots grown under different NH_4^+ and Pi conditions.

Treatment NH_4^+-Pi (mM)	WT	*nla*	*pho2*
	nmole/mg fresh weight		
10-10	28.8±3.1cd	171±18.1ab	177±18.8ab
3-10	30.2±3.4c	201±21.4a	206±23.2a
10-3	23.6±2.4d	148±15.8b	156±16.4b
3-3	24.5±2.7cd	162±16.8b	166±17.2ab

Pi content was measured at 27 days after sowing. Shown are mean ± SD. Values with different letters indicate significant difference at $P<0.05$.
doi:10.1371/journal.pgen.1002021.t004

Discussion

The identification of the *nla* suppressors as *phf1* and *pht1.1* and analysis of Pi levels in the *nla* mutant grown under different N and Pi regimes demonstrated that *NLA* has a role in regulating Pi homeostasis in plants. Further, the expression of *NLA* itself is regulated by a miR827 in a Pi dependent manner. Interestingly, comparing the phenotype of the *nla* and *pho2* mutants has shown a similar phenotypic pattern under varying NO_3^- and Pi regimes and both mutants overaccumulate Pi under low NO_3^- and high Pi conditions. Figure 5 shows the proposed model for the maintenance of Pi homeostasis via the regulation by the *NLA* and *PHO2* genes and the crosstalk between NO_3^- and Pi. The *NLA* and *PHO2* genes, along with higher NO_3^- applications, suppress Pi uptake in *Arabidopsis* WT plants. Plants grow normally as long as both NO_3^- and Pi supplies are sufficient, whereas, if either of them is limiting, plants start to accumulate anthocyanin as a stress symptom (Figure 5A). In the *nla* or *pho2* mutants, uptake of Pi is higher than in WT. However, when suppression by NO_3^- is also minimal when plants are grown under low NO_3^- and high Pi conditions, Pi accumulation is accelerated to toxic levels leading to necrotic senescence (Figure 5B). Thus, these mutants can grow

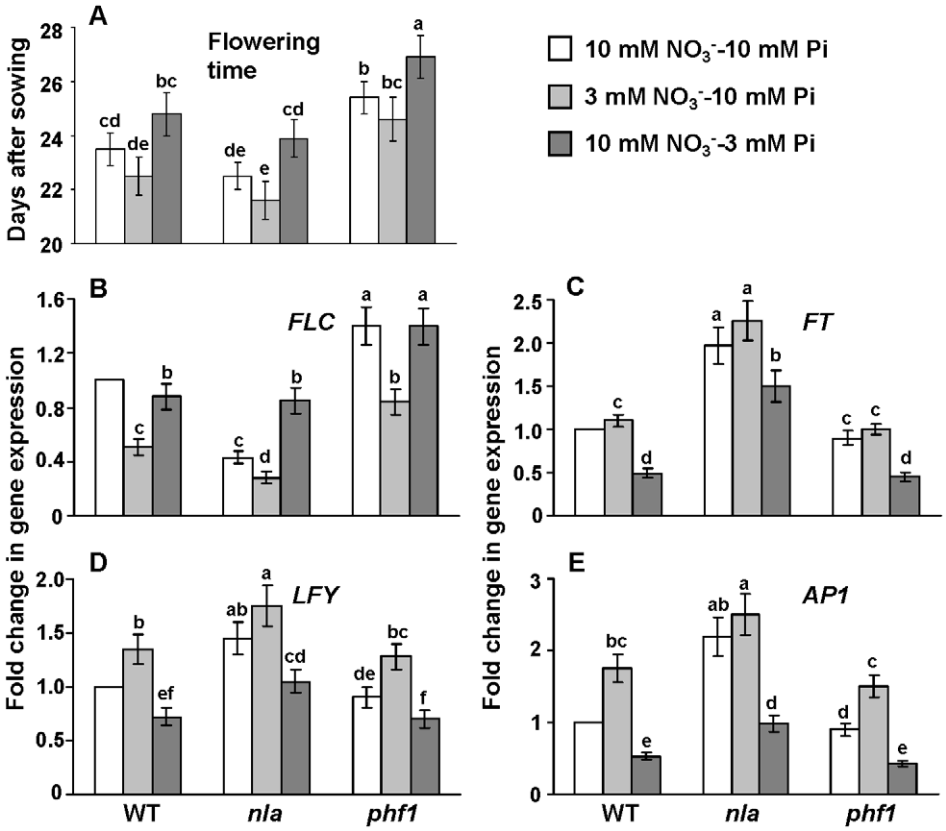

Figure 4. Effect of nitrate and phosphate regimes on flowering in *Arabidopsis.* (A) Flowering time (days after sowing), (B, C, D, and E) The relative expression of *FLC*, *FT*, *LFY*, and *AP1* genes, respectively, in leaves of WT, *nla* and *phf1* plants. Total RNA was extracted from leaves of plants harvested at 18 days after sowing. Relative transcript levels were determined by real-time PCR. Shown are mean ± SD. Bars with different letters indicate significant difference at $P<0.05$.
doi:10.1371/journal.pgen.1002021.g004

normally even when Pi supply is sub-optimal, without showing Pi deficiency symptoms (Figure 5B) and would have optimal internal Pi content in shoots (Table 1).

NO_3^- and Pi supply had antagonistic interactions for their accumulation in plants. However, the suppression by a higher supply of NO_3^- on Pi accumulation was larger than the suppression by higher supply of Pi on N content (Table 1 and Table S4). This could be due to two reasons, first that NO_3^- might have preferential uptake over Pi, since the requirement for N (>1% of dry matter) by most plants is usually higher than for P (<0.5% of dry matter). Second, the NO_3^- uptake system might not require negative regulators, since overaccumulation of N is not toxic to the plants and excess NO_3^- is stored in the vacuoles [33]. In contrast, *NLA* and *PHO2* serve as negative regulators of the Pi uptake system and are in turn regulated by miRNAs, which is necessary for the plants to avoid Pi toxicity caused by its overaccumulation. Further, the antagonistic interaction between NO_3^- and Pi was reflected by their inverse effect on flowering time in *Arabidopsis*, given that the plants flowered early under low-N conditions and it took a longer time to flower under low-Pi conditions (Figure 4A and Figure 5). Delayed flowering by low-Pi level could be via gibberellin signalling, since low gibberellin levels are known to delay flowering [32] and Pi and gibberellin levels are positively correlated [31]. In contrast, the plants flowered early under low NO_3^- conditions which could be either through a general stress management strategy to complete the life cycle earlier or through direct N affects on the flowering pathways. In agreement with the antagonistic crosstalk between NO_3^- and Pi for their uptake and inverse effects on flowering time observed here, the contrasting effects of NO_3^- and Pi on root architecture in *Arabidopsis* were reported earlier [34]. In that case, the primary root length decreased with increasing NO_3^- supply and increased with increasing Pi availability.

NLA is an E3 ligase and PHO2 is an E2 conjugase protein. The *Arabidopsis* genome contains 37 E2 and ~1300 E3 genes [35] and their proteins have potential roles for ubiquitination of target proteins destined to be degraded by the ubiquitin-26S proteasome. This pathway is employed by plants for the degradation and removal of proteins to maintain optimal growth and development. It would be interesting to study how NLA and PHO2 proteins interact to coordinate signals that specify the target proteins involved in Pi acquisition. *PHF1* and *PHT1.1* are likely direct or indirect targets of NLA and PHO2. This is supported by our results that mutations of *phf1* or *pht1.1* in the *nla* and *pho2* mutant background successfully reduced Pi overaccumulation and restored their Pi contents similar to WT. The *nla* mutant had high Pi accumulation while the OX-*NLA* plants do not have a significantly lower Pi than does WT (Table 1). The simplest explanation is that once a threshold level of NLA is reached, then increasing NLA does not change phenotype with regards Pi accumulation. In addition, NLA is an E3 ubiquitin ligase which is part of the E1–E2–E3 ubiquitination pathway to target proteins that are degraded by the 26S proteasome pathway. Hence, the co-ordination of both pathways might be necessary for the complete degradation of

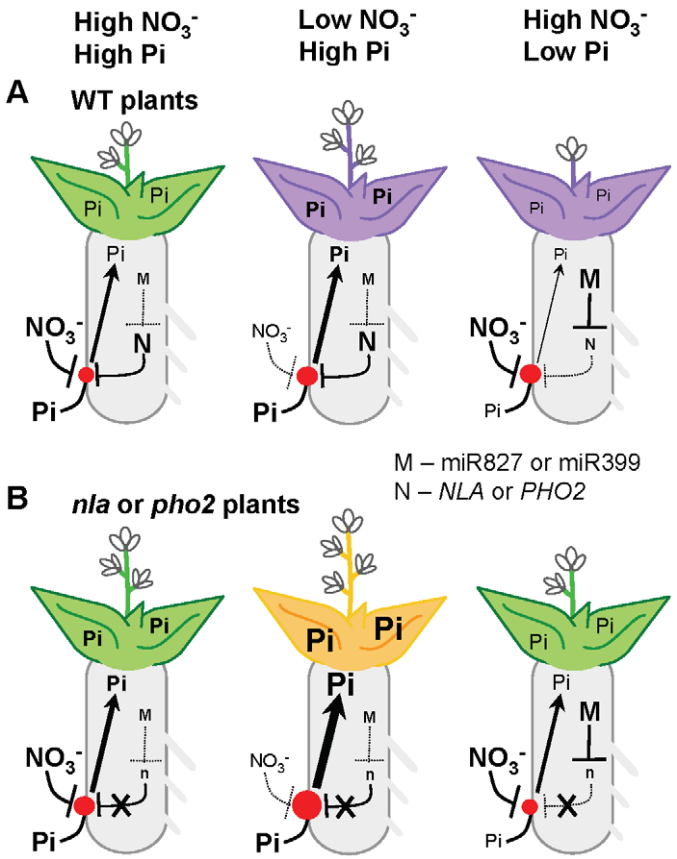

Figure 5. Hypothetical model for the role of *NLA* and *PHO2* genes and crosstalk between NO_3^- and Pi. (A) In WT plants, *NLA* and *PHO2* act as repressors for Pi uptake and Pi has a negative interaction with external NO_3^-. The condition of low NO_3^- and high Pi is most conducive for higher Pi uptake. (B) In *nla* or *pho2* mutants, the *NLA* or *PHO2* gene is not functional and these plants have higher Pi uptake compared to WT plants. Low NO_3^- and high Pi conditions accelerate Pi accumulation causing Pi toxicity in these mutants. Further, NO_3^- and Pi content has antagonistic affects on flowering time. Purple leaves show Pi deficiency leading to anthocyanin accumulation, orange leaves indicate Pi toxicity, solid red circles indicate the Pi uptake system and dotted lines indicate less suppression. The size of the letter 'Pi' in leaves and arrow thickness in roots is correlated with Pi content in plants.
doi:10.1371/journal.pgen.1002021.g005

PHF1 and PHT1.1 to a level which can significantly reduce the Pi content in OX-*NLA* plants, compared to WT plants. The role of *NLA* and *PHO2* in Pi homeostasis is further supported in that they are regulated by the low-Pi induced miRNAs, miR827 (Figure 2) and miR399 [18,19], respectively. The miR827 and miR399 are expressed at low levels under high-Pi conditions with the concomitant higher expression of *NLA* and *PHO2*. This is necessary to prevent the overloading of Pi into plants. Under low-Pi supply, increased expressions of miRNAs repress *NLA* and *PHO2* transcript levels and the repression of Pi transporters is alleviated (Figure 5). Given that Pi availability in soil is usually limited, this insures that sufficient Pi accumulation occurs in plants.

Over the next 50 years, it will be essential to increase crop yields by almost double to meet the needs of the growing world population. Increasing fertilizer use for higher crop yields would lead to large economic costs and vastly add to the environmental load of crop production. Therefore, the development of crops with improved genetics for nutrient use efficiency is absolutely crucial for the sustainability of crop production. We have demonstrated that *NLA* and *PHO2* (their regulation by miR827 and miR399) have pivotal roles in NO_3^- regulated control of Pi homeostasis. In fertilized agricultural soils, Pi availability is typically low when compared to NO_3^-, although more fixed N is required for maximal plant growth. It should be possible by modulating the expression of *NLA* or *PHO2* to develop crop cultivars that better utilize the available P in balance with N supply.

Materials and Methods

Plant Material and Growth Conditions

Arabidopsis thaliana ecotype Columbia was used in the experiments unless otherwise stated. The seeds were stratified at 4°C for 3 d and sown in nutrient-free LB2 soil (SunGro Horticulture Canada Ltd, http://www.sungro.com/). The plants were grown in controlled growth chambers at 16 h light/8 h dark, 23°C day/18°C night, light intensity 200 µE m^{-1} s^{-1} and 65% relative humidity. The nutrient solution was applied once a week for 4 weeks and contained 2 mM $MgSO_4$, 1 mM $CaCl_2$, 100 µM Fe-EDTA, 50 µM H_3BO_3, 12 µM $MnSO_4$, 1 µM $ZnCl_2$, 1 µM $CuSO_4$ and 0.2 µM Na_2MoO_4. N and P were supplied in the form of KNO_3 and KH_2PO_4 (pH 6.0), respectively, with varying concentration as mentioned in the results. The nutrient levels used in the experiments are relative levels, but not absolute levels. To avoid the discrepancies of maintaining the absolute nutrient levels in soil between different experiments, we have previously developed the defined nutrient growth conditions [21]. The application of nutrient solution once every week for 4 weeks to *Arabidopsis* with varying N supplies showed that 10 mM NO_3^- is

sufficient-N for optimum plant growth and yield, 3 mM NO_3^- is moderately low-N where plants start to develop adaptive responses required to deal with low-N conditions and 1 mM NO_3^- is a severe-N limiting condition [21] (Figure S5A). The varying P levels showed that 10 mM Pi is sufficient-P for optimum plant growth and yield, 3 mM Pi is moderately low to sufficient-P with a slight appearance of red color in leaves indicating the start of anthocyanin accumulation, 1 mM Pi is a moderately low-P condition with higher anthocyanin accumulation and significantly lower plant growth and yield and 0.5 mM Pi is a severe-P limiting condition (Figure S5B). Shoots and roots were harvested separately at the indicated days, frozen in liquid nitrogen and stored at −80°C until use. The T-DNA insertion mutant lines for different genes obtained from the *Arabidopsis* Biological Resource Center and used in the experiments are: *phf1* (SALK_144943), *pht1.1* (SALK_088586), *pht1.4* (SALK_103881), *pht2.1* (SALK_094069), *siz1* (SALK_065397), *phr1* (SALK_067629), and miR827 (SALK_020837).

Isolation of *nla* Mutant Suppressors and Positional Cloning

The homozygous *nla* mutant (in Col background) seeds were soaked overnight at 4°C in 100 mM phosphate buffer pH 7.5 and then treated with 0.4% ethyl methanesulfonate (EMS) for 8 h at room temperature. The seeds were washed thoroughly and sown in LB2 soil supplied with 3 mM KNO_3^- and 10 mM KH_2PO_4 and other nutrients as above. The M1 plants were grouped into 120 sets, with each set having a pool of 36–40 plants. The seeds from each set were harvested separately. About 200 M2 plants within each set were grown on 3 mM KNO_3^- and 10 mM KH_2PO_4 to screen for putative *nla*-suppressor plants which would recover the *nla* mutant phenotype similar to WT. Two putative *nla*-suppressors (*nla-sup1* and *nla-sup2*) plants were identified and were backcrossed twice with *nla*-Col mutant plants. Simultaneously, to achieve the *nla* mutation in Ler genetic background, the homozygous *nla*-Col plant was crossed with Ler WT plant and the *nla*-Ler plant obtained from this cross was further backcrossed nine times with Ler WT plant to produce genetically clean *nla*-Ler. The *nla*-suppressor-Col plant was crossed with *nla*-Ler plant. Among the segregating F2 progeny, which was grown at 3 mM KNO_3^- and 10 mM KH_2PO_4, ~500 plants showing the WT phenotype were selected for mapping. The first round of mapping was performed as described by Luckowitz et al. [36]. The second round of fine mapping was accomplished using the simple sequence length polymorphism (SSLP) markers prepared from the *Arabidopsis* genome sequence (www.arabidopsis.org). The mapping schemes are shown in Figure 1. We identified two independent putative *nla*-suppressors, with the mapping for each done separately. One suppressor, *nla-sup1*, was linked to the *PHF1* (At3g52190) gene and the other, *nla-sup2*, was linked to the *PHT1.1* (At5g43350) gene.

Plant Transformation

For the complementation and overexpression analysis, the coding and/or genomic sequences of *NLA* (At1g02860), *PHF1* and *PHT1.1* genes and a 300 bp region including miR827 sequences were amplified by PCR and cloned into gateway-compatible vectors pEarleyGate 100 and/or pEarleyGate 101 [37]. The plasmids were transformed into *Agrobacterium tumefaciens* strain EHA105 and then transformed into WT Col, *nla-sup1*, *nla-sup2*, *nla* and/or *pho2* plants as described by Clough and Bent [38]. The transgenic plants were selected with the herbicide selection BASTA (active ingredient glufosinate ammonium). Five independent OX lines carrying a single transgene copy for all the constructs were generated. At least two independent lines for each construct were used in the experiments and representative data of one OX line is given in the results.

Biochemical Assays

Frozen shoot and root tissue was used for the following biochemical assays. Pi and total P contents were measured as described by Chiou et al. [18], which is originally adapted from the protocol mentioned by Ames [39]. The percentage of total N in the dried tissues was measured by the Micro-Dumas combustion analysis method using a Carlo Erba NA1500 C/N analyzer, (Carlo Erba Strumentazione, Milan, Italy).

Pi Uptake Assay

The plants were grown for 12 day on agar plates (1% sucrose and 0.8% agar) with 1 mM KNO_3 and 0.5 mM KH_2PO_4 with the other nutrient concentrations the same as in the soil experiments. Ten plants were pooled and roots were immersed in 7 ml nutrient solution, except with the replacement of KH_2PO_4 by [^{33}P]orthophosphate (10.2×10^{-2} MBq/7 ml; Perkin-Elmer). The plants were incubated for 2 and 4 h and then rinsed with nutrient solution without ^{33}P. The plants were weighed and lysed in 500 µl of 30% H_2O_2 and 200 µl of perchloric acid for 1 h at 70°C and 5 ml scintillation liquid was added to each sample, incubated over night and the activity measured by scintillation counter.

Quantitative Real-Time PCR

Total RNA was isolated using TRIZOL reagent (Invitrogen, Carlsbad, CA, USA). To eliminate any residual genomic DNA, total RNA was treated with RQ1 RNase-free DNase (Promega, Madison, WI, USA). The cDNA was synthesized from total RNA by using the Reverse Transcription System kit (Promega). Primer Express 2.0 software (Applied Biosystems, Forster City, CA, USA) was used to design the primers. Primer sequences for each gene are given in Table S5. Real-time PCR was performed as described previously [40]. Relative quantification (RQ) values for each target gene were calculated by the $2^{-\Delta\Delta CT}$ method [41] using *UBIQUITIN10* (*UBQ10*) and/or *GLYCERALDEHYDE 3-PHOSPHATE DEHYDROGENASE A SUBUNIT* (*GAPA*) as an internal reference gene. To ensure the validity of the $2^{-\Delta\Delta CT}$ method, twofold serial dilutions of cDNA were used to create standard curves, and the amplification efficiencies of the target and reference genes shown to be approximately equal.

Statistical Analysis

Statistical analysis was done by Fisher's protected LSD test using SAS statistical software (SAS Institute, Inc., NC). The results shown are representative of three independent experiments and within each experiment treatments were replicated three times, unless otherwise stated.

Supporting Information

Figure S1 Effect of nitrate and phosphate regimes on growth of *Arabidopsis* WT, *nla-sup2*, *OX-NLA*, *nla* and *pho2* plants. Plants grown at (A, C) 10 mM NO_3^--10 mM Pi, and (B, D) 3 mM NO_3^--10 mM Pi conditions.
(TIF)

Figure S2 Effect of nitrate and phosphate regimes on growth of *Arabidopsis* WT and *nla* plants. Plants grown at (A) 10 mM NO_3^--

10 mM Pi, (B) 3 mM NO_3^--10 mM Pi, and (C) 10 mM NO_3^--3 mM Pi conditions.
(TIF)

Figure S3 Effect of nitrate and phosphate regimes on growth of *Arabidopsis* WT and *nla* (ecotype Wassilewskija, Ws) plants. Plants grown at (A) 10 mM NO_3^--10 mM Pi, and (B) 3 mM NO_3^--10 mM Pi conditions.
(TIF)

Figure S4 Effect of ammonium and phosphate regimes on growth of *Arabidopsis* WT and *nla* plants. Plants at (A) 20 days after sowing, and (B) 28 days after sowing.
(TIF)

Figure S5 Effect of varying N (A) and P (B) regimes on growth of *Arabidopsis* WT plants.
(TIF)

Table S1 Pi content in *Arabidopsis* shoots.
(DOC)

Table S2 Pi content in *Arabidopsis* roots.
(DOC)

Table S3 Pi content in *Arabidopsis* roots and inflorescence.
(DOC)

Table S4 Total nitrogen content in *Arabidopsis* WT plants.
(DOC)

Table S5 Primers used for real-time PCR analysis of gene expression.
(DOC)

Acknowledgments

We thank Yuhai Cui for guidance in map-based cloning. We greatly thank Drs. Yves Poirier, Tzyy-Jen Chiou, Javier Paz-Ares, Antonio Leyva, Tara Narwani, Dae-Jin Yun, and the *Arabidopsis* Biological Resource Center (ABRC) for kindly providing mutant seeds of *pho1*, *pho2*, *phf1*, *pht1.1*, *phr1*, *siz1*, and T-DNA insertion mutant lines. We thank Jaideep Mathur, Joseph Colasanti, and Yong Mei Bi for critical reading of the manuscript and Benjamin Jull and Sabrina Humbert for help with plant care and sampling.

Author Contributions

Conceived and designed the experiments: SK SJR. Performed the experiments: SK MP. Analyzed the data: SK. Contributed reagents/materials/analysis tools: SK SJR. Wrote the paper: SK SJR.

References

1. Poirier Y, Bucher M (2002) Phosphate transport and homeostasis in *Arabidopsis*; Somerville CR, Meyerowitz E, eds. American Society of Plant Biologists. Rockville, MD, doi:10.1199/tab.0024, http://www.aspb.org/publications/Arabidopsis.
2. Marschner H (1995) Mineral nutrition of higher plants. London: Academic Press.
3. Good AG, Shrawat AK, Muench DG (2004) Can less yield more? Is reducing nutrient input into the environment compatible with maintaining crop production? Trends Plant Sci 9(12): 597–605.
4. Barber SA, Walker JM, Vasey EH (1963) Mechanisms for movement of plant nutrients from soil and fertilizer to plant root. J Agri Food Chem 11(3): 204–207.
5. Raghothama KG (1999) Phosphate acquisition. Annu Rev Plant Physiol Plant Mol Biol 50: 665–693.
6. Lin WY, Lin SI, Chiou TJ (2009) Molecular regulators of phosphate homeostasis in plants. J Exp Bot 60(5): 1427–1438.
7. Rubio V, Linhares F, Solano R, Martin AC, Iglesias J, et al. (2001) A conserved MYB transcription factor involved in phosphate starvation signaling both in vascular plants and in unicellular algae. Genes Dev 15(16): 2122–2133.
8. Miura K, Rus A, Sharkhuu A, Yokoi S, Karthikeyan AS, et al. (2005) The *Arabidopsis* SUMO E3 ligase SIZ1 controls phosphate deficiency responses. Proc Natl Acad Sci USA 102(21): 7760–7765.
9. Gonzalez E, Solano R, Rubio V, Leyva A, Paz-Ares J (2005) PHOSPHATE TRANSPORTER TRAFFIC FACILITATOR1 is a plant-specific SEC12-related protein that enables the endoplasmic reticulum exit of a high-affinity phosphate transporter in *Arabidopsis*. Plant Cell 17(12): 3500–3512.
10. Shin H, Shin HS, Dewbre GR, Harrison MJ (2004) Phosphate transport in *Arabidopsis*: Pht1;1 and Pht1;4 play a major role in phosphate acquisition from both low- and high-phosphate environments. Plant J 39(4): 629–642.
11. Mitsukawa N, Okumura S, Shirano Y, Sato S, Kato T, et al. (1997) Overexpression of an Arabidopsis thaliana high-affinity phosphate transporter gene in tobacco cultured cells enhances cell growth under phosphate-limited conditions. Proceedings of the National Academy of Sciences of the United States of America 94(13): 7098–7102.
12. Versaw WK, Harrison MJ (2002) A chloroplast phosphate transporter, PHT2;1, influences allocation of phosphate within the plant and phosphate-starvation responses. Plant Cell 14(8): 1751–1766.
13. Duan K, Yi KK, Dang L, Huang HJ, Wu W, et al. (2008) Characterization of a sub-family of *Arabidopsis* genes with the SPX domain reveals their diverse functions in plant tolerance to phosphorus starvation. Plant J 54(6): 965–975.
14. Hamburger D, Rezzonico E, Petetot JMC, Somerville C, Poirier Y (2002) Identification and characterization of the *Arabidopsis PHO1* gene involved in phosphate loading to the xylem. Plant Cell 14(4): 889–902.
15. Wang Y, Ribot C, Rezzonico E, Poirier Y (2004) Structure and expression profile of the Arabidopsis PHO1 gene family indicates a broad role in inorganic phosphate homeostasis. Plant Physiology 135(1): 400–411.
16. Poirier Y, Thoma S, Somerville C, Schiefelbein J (1991) A Mutant of Arabidopsis Deficient in Xylem Loading of Phosphate. Plant Physiology 97(3): 1087–1093.
17. Aung K, Lin SI, Wu CC, Huang YT, Su CL, et al. (2006) pho2, a phosphate overaccumulator, is caused by a nonsense mutation in a MicroRNA399 target gene. Plant Physiol 141(3): 1000–1011.
18. Chiou TJ, Aung K, Lin SI, Wu CC, Chiang SF, et al. (2006) Regulation of phosphate homeostasis by microRNA in *Arabidopsis*. Plant Cell 18(2): 412–421.
19. Fujii H, Chiou TJ, Lin SI, Aung K, Zhu JK (2005) A miRNA involved in phosphate-starvation response in *Arabidopsis*. Curr Biol 15(22): 2038–2043.
20. Crawford NM, Forde BG (2002) Molecular and developmental biology of inorganic nitrogen nutrition.; Somerville CR, Meyerowitz E, eds. American Society of Plant Biologists. Rockville, MD, doi:10.1199/tab.0011, http://www.aspb.org/publications/Arabidopsis.
21. Peng M, Hannam C, Gu HL, Bi YM, Rothstein SJ (2007) A mutation in *NLA*, which encodes a RING-type ubiquitin ligase, disrupts the adaptability of *Arabidopsis* to nitrogen limitation. Plant J 50(2): 320–337.
22. Peng M, Hudson D, Schofield A, Tsao R, Yang R, et al. (2008) Adaptation of *Arabidopsis* to nitrogen limitation involves induction of anthocyanin synthesis which is controlled by the NLA gene. J Exp Bot 59(11): 2933–2944.
23. Chalker-Scott L (1999) Environmental significance of anthocyanins in plant stress responses. Photochemistry and Photobiology 70(1): 1–9.
24. Carrington JC, Ambros V (2003) Role of microRNAs in plant and animal development. Science 301(5631): 336–338.
25. Bartel DP (2004) MicroRNAs: Genomics, biogenesis, mechanism, and function. Cell 116(2): 281–297.
26. Pant BD, Musialak-Lange M, Nuc P, May P, Buhtz A, et al. (2009) Identification of nutrient-responsive *Arabidopsis* and rapeseed microRNAs by comprehensive real-time polymerase chain reaction profiling and small RNA sequencing. Plant Physiol 150(3): 1541–1555.
27. Jones JB (1998) Phosphorus toxicity in tomato plants: When and how does it occur? Commun Soil Sci Plant Analysis 29(11-14): 1779–1784.
28. Delhaize E, Randall PJ (1995) Characterization of a phosphate-accumulator mutant of *Arabidopsis thaliana*. Plant Physiol 107(1): 207–213.
29. Tinker PB, Nye PH (2000) Solute movement in the rhizosphere: Oxford: Oxford University Press.
30. Mouradov A, Cremer F, Coupland G (2002) Control of flowering time: Interacting pathways as a basis for diversity. Plant Cell 14: S111–S130.
31. Jiang C, Gao X, Liao L, Harberd NP, Fu X (2007) Phosphate starvation root architecture and anthocyanin accumulation responses are modulated by the gibberellin-DELLA signaling pathway in *Arabidopsis*. Plant Physiol 145(4): 1460–1470.
32. Blazquez MA, Green R, Nilsson O, Sussman MR, Weigel D (1998) Gibberellins promote flowering of *Arabidopsis* by activating the LEAFY promoter. Plant Cell 10(5): 791–800.

33. De Angeli A, Monachello D, Ephritikhine G, Frachisse JM, Thomine S, et al. (2006) The nitrate/proton antiporter AtCLCa mediates nitrate accumulation in plant vacuoles. Nature 442(7105): 939–942.
34. Linkohr BI, Williamson LC, Fitter AH, Leyser HMO (2002) Nitrate and phosphate availability and distribution have different effects on root system architecture of *Arabidopsis*. Plant J 29(6): 751–760.
35. Smalle J, Vierstra RD (2004) The ubiquitin 26S proteasome proteolytic pathway. Annu Rev Plant Biol 55: 555–590.
36. Lukowitz W, Gillmor CS, Scheible WR (2000) Positional cloning in *Arabidopsis*. Why it feels good to have a genome initiative working for you. Plant Physiol 123(3): 795–805.
37. Earley KW, Haag JR, Pontes O, Opper K, Juehne T, et al. (2006) Gateway-compatible vectors for plant functional genomics and proteomics. Plant J 45(4): 616–629.
38. Clough SJ, Bent AF (1998) Floral dip: a simplified method for Agrobacterium-mediated transformation of *Arabidopsis thaliana*. Plant J 16(6): 735–743.
39. Ames BN (1966) Assay of inorganic phosphate, total phosphate and phosphatases. Methods Enzymol 8: 115–118.
40. Kant S, Kant P, Raveh E, Barak S (2006) Evidence that differential gene expression between the halophyte, *Thellungiella halophila*, and *Arabidopsis thaliana* is responsible for higher levels of the compatible osmolyte proline and tight control of Na^+ uptake in *T. halophila*. Plant Cell Environ 29(7): 1220–1234.
41. Livak KJ, Schmittgen TD (2001) Analysis of relative gene expression data using real-time quantitative PCR and the $2^{-\Delta\Delta CT}$ method. Methods 25(4): 402–408.